RSC Advances

ROYAL SOCIETY OF CHEMISTRY

www.rsc.org/advances

Journal Name

ARTICLE

Hierarchically Mesoporous/macroporous Structured TiO_2 for Dye-Sensitized Solar Cells

Received 00th January 20xx,
Accepted 00th January 20xx

DOI: 10.1039/x0xx00000x

www.rsc.org/

Dianyu Qi,[a] Lingzhi Wang*[a] and Jinlong Zhang*[a b]

In this study, hierarchical TiO_2 with macro- and mesostructure is prepared and applied in Dye-sensitized solar cell (DSSCs). To achieve the hierarchical structure, hard and soft tamplating is combined. Polystyrene spheres serve as the hard template for μm-scale macropores, and triblock copolymers act as the soft template of nm-scale mesopores. The prepared hierarchical TiO_2 is analyzed by TEM, XRD and N_2 sorption, and results indicate meso/macroporous structure are successfully obtained. Mesoporous structure provides a larger surface area for dye adsorption, and macroporous structure induces a faster electron transportation property. Combining the advantages of mesopore and macropore, the prepared hierarchical TiO_2 DSSCs shows a higher photon to electron efficiency in comparison to individual mesoporous and macroporous sample.

Introduction

Energy crisis has become a worldwide problem during the past decades because of the exhaustion of fossil energy. Because of pollution-free and inexhaustible, solar energy is a promising solution to solve the problem. Solar cell is a typical way to take use of the solar energy, and it has been widely studied and applied in our daily lives. Traditional silicon-based solar cell is high-cost because of the demand for ultra-high purity silicon. Dye-sensitized solar cell (DSSCs) has advantage such as low cost and easy fabrication, and it has drawn more and more attentions of researchers.[1-5]

In DSSCs devices, a layer of semiconductor (mostly TiO_2) is necessary and has a significant effect on the power conversion efficiency. The semiconductor layer serves as the support of the dye sensitizers, collector of the electrons and the bridge for charge transfer. Therefore, the semiconductor layer should provide large surface area and fast charge transfer efficiency. The former supplies more sites for dye adsorption, and the latter can reduce the energy loss from the recombination of photocharges in transfer process. Researchers have done a lot of work on the morphology of the semiconductor material and then improved the power conversion efficiency of DSSCs.[4, 6, 7] Take TiO_2 semiconductor as an example, to improve the adsorption of dye, mesoporous or nanocrystal TiO_2 have been developed.[2, 8, 9] To suppress the recombinations of the photocharges, morphologies suit for charge transportation have been developed, such as single crystal,[10, 11] nanotube,[12, 13] nanorod[14, 15] and macroporous structure.[16-18] Moreover, hierarchical structures tend to achieve a higher efficiency.[19-21] Edward reported mesoporous single crystal TiO_2 and applied it in DSSCs, the prepared DSSCs presented much higher efficiency.[22] Zhang developed 1D nanorods into hierarchical branch-like structure and enhanced the performance of DSSCs.[6] Liao prepared hierarchical TiO_2 by combining nanoribbons and microspheres structures, resulting in fast electron transportation and longer electron lifetime.[23] In general, hierarchical structures improve DSSCs performances mainly due to following two reasons: (i) increased surface area improves the dye adsorption; (ii) faster electron transportation leads to the inhibition of charge recombinations.

Therefore, in this study, we fabricated a novel hierarchical (mesoporous/ macroporous) structure for the application in DSSCs. We aim at combining the advantages of the mesoporous and macroporous structure, which means more dye adsorption ability induced by mesopores and faster electron transportation property induced by macropores. Here, the hierarchical (mesoporous/ macroporous) TiO_2 is prepared by respectively using polystyrene spheres and triblock copolymer molecules as the templates of mesopores and macropores. As reference samples, individual mesoporous TiO_2 and macroporous TiO_2 are also synthesized. The hierarchical samples shows more dye adsorption ability and faster charge transfer property. As a result, hierarchical TiO_2 DSSCs shows higher photon to electron conversion efficiency.

Experimental Section

Synthetic procedures

The preparation of mesoporous titania (Mes-TiO_2): Mesoporous titania was prepared according to the reported sol-gel method.[24] In a typical synthesis, 5.6 mL of titanium

[a] Key Laboratory for Advanced Materials and Institute of Fine Chemicals, East China University of Science and Technology, 130 Meilong Road, Shanghai 200237, P. R. China.
[b] Department of Chemistry, Tsinghua University, Beijing 100084, P. R. China

isopropoxide (TTIP), 1 mL of acetylacetone, 0.83 mL of hydrochloric acid and 4.6 mL of H_2O were added to 50 mL of ethanol under moderate stirring. After stirring 2 h, 1.03 g of Triblock copolymer Pluronic F127 (EO_{106}-PO_{70}-EO_{106}) was added to the solution and dissolved at 45 °C. After stirring 1 h, the sol was transferred into petri-dishes and kept at 40 °C for 24 h and then 80 °C for 24h. After that, the obtained gel was calcined at 450 °C for 2 h, and the obtained white powder is Mes-TiO_2.

The preparation of mesoporous/macroporous titania (Hier-TiO_2): Hierarchical titania was synthesized by using F127 and polystyrene sphere (PS) as the template for mesopores and macropores. PS colloidal suspension (340 nm) was synthesized according to our previous work.[25] PS colloidal suspension was mixed with the mentioned precursor solution of mes-TiO_2 according to volume ratio of 3:1 under vigorous stirring for 5 min. The mixture was poured into a petri-dish, and then transferred into a 40 °C oven for 24 h, and then 80 °C for 24h. After that, the obtained solid was calcined at 450 °C for 2 h, giving Hier-TiO_2 as white powder.

The preparation of macroporous titania (Mac-TiO_2): The synthesis process of macroporous titania is almost same as that of hierarchical titania, except for no addition of F127 in the process.

Fabrication of Dye-sensitized solar cells: The fabrication of DSSCs was achieved according to the reported reference.[3] To form a block layer of the photoanode, FTO glass were immersed in $TiCl_4$ (40 mM) solution at 70 °C for 30 min and then washed repeatedly. Three kinds of titania (Mes-, Hier-, Mac-TiO_2) were applied to prepare the screen-printing pastes. To form the transparent layer of the photoanode, these pastes were coated on the TiO_2 blocked FTO by screen-printing (mesh count: 300T mesh/inch, scale: 5 mm × 5 mm). In screen-printing process, the procedure was repeated to obtain an appropriate thickness (12-14 μm), and the flatting time is 5 min and drying temperature is 125 °C for each time. There is no light-scattering layer in this process. The electrodes were heated at 500 °C for 30 min. After cooling down, the electrodes were immersed again in $TiCl_4$ (40 mM) solution at 70 °C for 30 min and then calcined at 500 °C for 30 min. When they were cooling to 80 °C, the TiO_2 electrodes were transferred quickly into cis-di(thiocyanato)-N-N'-bis(2,2'-bipyridyl-4-carboxylic acid-4'-tetrabutylammonium carboxylate) ruthenium(II) (N719) dye solution (0.5 mM) of acetonitrile and tetrabutyl alcohol (volume ratio 1:1), and kept at 25 °C for 24 h. As a result, three kinds of TiO_2 photoanode were prepared.

To prepare the counter Pt electrode, a hole with 0.8 mm diameter was drilled on the FTO glass. After that, the drilled FTO glasses were washed repeatedly by water and ethanol. The cleaned FTO glasses were coated by a drop (10 μL) of H_2PtCl_6 solution. After flatting, the electrodes were heated at 150 °C for 10 min and then 400 °C for 15 min.

To assemble a solar cell, the prepared photoanode and Pt electrode were sealed with a hot-melt Surlyn 1702 ring (45 μm) with an open area (7 mm × 7 mm) at 125 °C for 20 s under 0.3 MPa pressure. After that, electrolyte was injected into the middle space and vacuum backfilling was applied to remove the inside air bubbles. The electrolyte was a solution of butylmethylimidazolium iodide (0.6 M), iodine (0.03 M), guanidinium thiocyanate (0.1 M) and 4-tertbutylpyridine (0.5 M) in the mixture of valeronitrile and acetonitrile (volume ratio, 15:85). At last, the hole was sealed with a small cover glass using hot-melt Surlyn. To decrease the contact resistance between solar cell and clips of measurement instrument, the edge of FTO outside is covered by a layer of silver.

Characterizations

X-ray powder diffraction (XRD) patterns were analyzed on Rigaku D/max 2550 VB/PC. Transmission electron microscopy (TEM) was performed on JEM-2100 to observe the morphologies of the titania. Scanning electron microscopy (SEM) was performed on TESCAN nova-3 to measure the thickness of the titania film (cross section). BET surface areas and nitrogen isotherms were recorded on Micromeritics ASAP 2020, and the samples were degassed in vacuum at 300 °C for 6 h. Dye adsorption ability measurements were performed as follows: At first, TiO_2 samples were immersed in above N719 solution for 2 days to achieve completely dye adsorption. Dye adsorbed TiO_2 were then washed by acetonitrile, dried and weighted. The weighted powders were dispersed into 20 mL eluent (0.1 M NaOH solution of ethanol and water, volume ratio is 1:1), and then kept shaking for 10 min to release the dye completely. After centrifuging, the concentrations of the dye solution are analyzed quantitatively by the UV-Vis spectrophotometer via standard curve method. Photovoltaic measurements were performed by using an AM1.5 sun simulator (NEWPORT 3A) as light source. Before measurement the power of the light was calibrated to 100 mW/cm^2 by using a reference Si solar cell. I-V curves were measured on ZAHNER electric potentiostat, and the voltage step was 10 mV and delay time was 40 ms. The electrochemical impedance spectroscopy (EIS) measurements were recorded over a frequency range of 0.1-100 KHz with ac amplitude of 10 mV.

Results and discussion

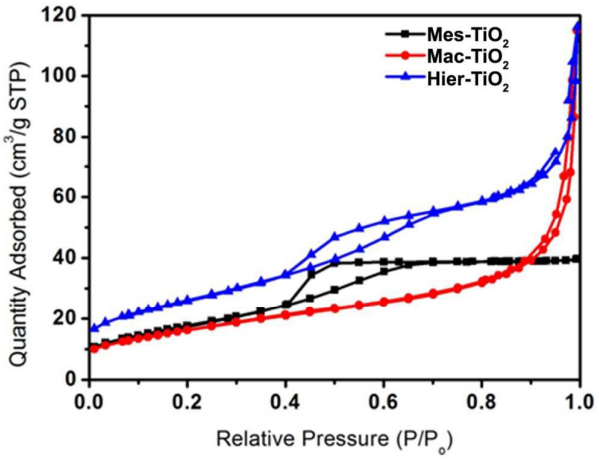

Figure 1. N_2 sorption curves of Hier-TiO_2, Mac-TiO_2 and Mes-TiO_2

Table 1. Parameters of Hier-TiO_2, Mac-TiO_2 and Mes-TiO_2 (calculated from isotherms)

Samples	Hier-TiO_2	Mac-TiO_2	Mes-TiO_2
BET surface area (m_2/g)	94	59	90
Pore diameter (nm)	3.4	--	3.3

Figure 1 shows the N_2 sorption isotherms of The TiO_2 samples. The curve of mes-TiO_2 presents an obvious hysteresis loop at the region of 0.4-0.6, proving the existence of mesoporous structure. Moreover, no abrupt change is observed at the high pressure region of 0.9-1.0, indicating that there is no macroporous structure in Mes-TiO_2 sample. In contrast, Mac-TiO_2 presents an opposite result, suggesting that there is no mesoporous but macroporous structure. In the case of Hier-TiO_2, the characters of mesopores and macropores are both observed, and it is obviously that the mesopores and macropores both exist in Hier-TiO_2 sample.

To further confirm the morphology of samples, transmission electron microscope was applied (Figure 2). In TEM images of Hier-TiO_2, it is obviously that the pore size of macropore is about 250 nm, which is obtained from the PS template. Because of the shrinkage in calcination, the pore is smaller than PS template sphere (340 nm). Moreover, on the walls of the macropores, there are lots of mesopores, which formed by the F127 template. The pore size of mesopores is about 3.4 nm, which is coincident with the result calculated from N_2 desorption isotherms (Table 1). In contrast, Mac-TiO_2 sample shows only macropores of 250 nm and Mes-TiO_2 sample presents only mesopores of 3.3 nm. The results confirm that mesoporous, macroporous and hierarchical titania were successfully prepared.

The X-ray diffraction patterns (XRD) of the samples are shown in Figure 3. Obviously, these three kinds of titania are all composed by anatase phase (Figure 3a), and the peaks around 25°, 38°, 48°, 54°, 55°, 63°and 75° are respectively attributed to the (101), 004), (200), (105), (211), (204) and (215) crystal phase of anatase (PDF#12-2172). Moreover, peak width at half height of Mes-TiO_2 sample is the smallest, indicating the crystal size of Mes-TiO_2 is the biggest, but crystal size of Mac- and Hier-TiO_2 are much smaller. This phenomenon can be explained by the isolation effect of PS template in titania crystal growing process.[25] From small angle XRD patterns of the samples (Figure 3b), it can be seen that the curve of Mes-TiO_2 presents a peak at 0.7°, which is same as that mentioned in reference.[24] Mes-TiO_2 presents the peak because of its long range ordered structure, but the length of mesoporous structure in Hier-TiO_2 is limited by the thickness of macropore wall, resulting in the absence of signal in small angle XRD pattern.

In DSSCs devices, dye adsorption ability is very important to the efficiency. Because of the difference in morphology and surface area, the samples may present different dye adsorption ability. To estimate the dye adsorption ability, dye-adsorbed TiO_2 were immersed in alkali solvent to release the dye completely. The N719 adsorption is attributed to the com-

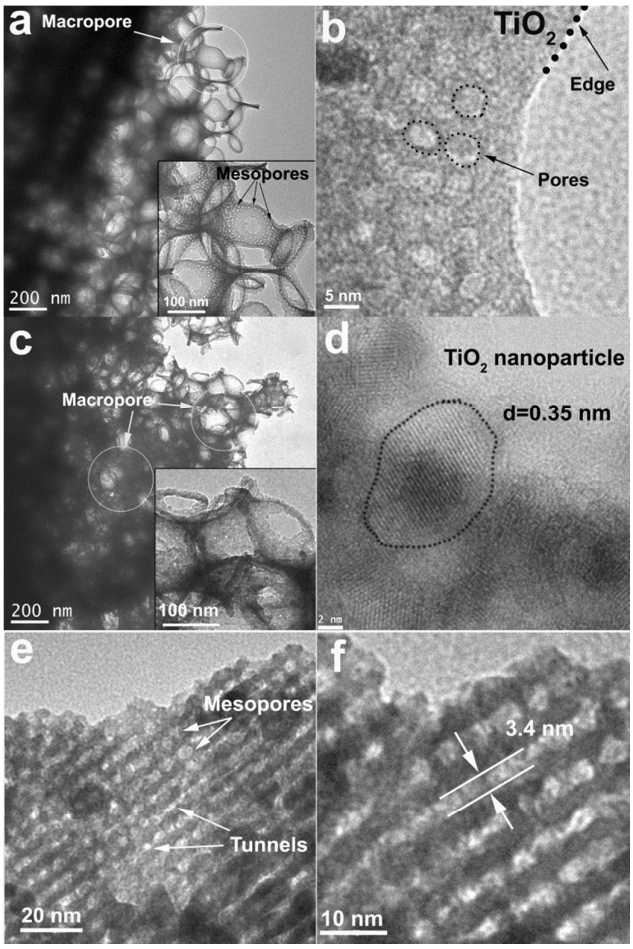

Figure 2. TEM images of Hier-TiO2 (a, b), Mac-TiO2 (c, d) and Mes-TiO2 (d, e)

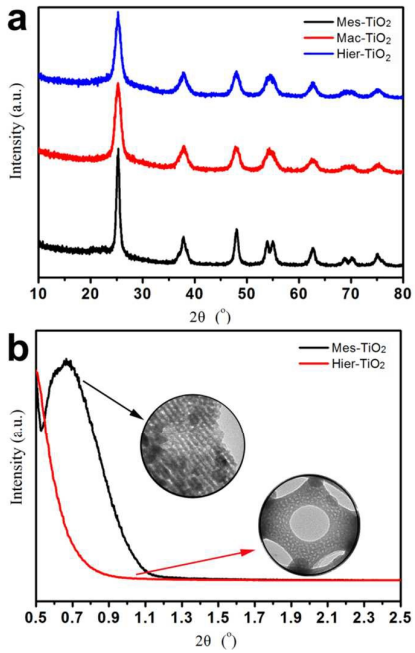

Figure 3. Wide angle (a) and small angle (b) XRD patterns of the samples

Table 2. The dye adsorption ability of the samples

Samples	Mes-TiO_2	Mac-TiO_2	Hier-TiO_2
Mass (g)	0.0945	0.128	0.104
Absorbance of dye solution	0.111	1.66	1.648
Dye adsorption ability (mmol/g)	0.07	0.772	0.943

bination of –COOH and –OH, which can be destroyed by alkali. Therefore, dye adsorbed on titania can be eluted and then quantified. The result is shown in Table 2. Obviously, Hier-TiO_2 shows the highest dye adsorption ability, which is attributed to the interconnected structure of macropores and the large surface area of mesopores. Obviously, Mes-TiO_2 sample has a large surface area but shows the lowest adsorption ability, which can be explained by the length of mesopores (Figure 4). Mes-TiO_2 has long straight mesoporous structure, and dye molecules tend to adsorb at the ends of mesopores. In result, mesopores will be blocked and the inner space will not adsorb dye molecules (Figure 4a). Therefore, Mes-TiO_2 shows very weak dye adsorption ability. In the case of Hier-TiO_2, the length of mesopores is reduced because of the thickness limit from macropore walls, resulting in further development of dye adsorption (Figure 4b). Mac-TiO_2 has macropores but no mesopores, and dye molecules are only adsorbed on the walls of macropores (Figure 4c). Thus, its dye adsorption ability is a little lower than Hier-TiO_2.

In order to evaluate the effect of hierarchical structure on DSSCs, three kinds of titania were all applied to assemble solar cells, and their photo to current conversion efficiencies are shown in I-V curves (Figure 5). Mes-TiO_2 presents the lowest efficiency, which due to its poor dye adsorption ability. Hier-TiO_2 and Mac-TiO_2 show higher open circuit potential, because of the charge collection effect of the interconnected macroporous structure.[21] Therefore, the charge transfer between photoanode and electrolyte can be promoted. To confirm the superiority of macroporous structure in charge transportation, the EIS spectra of the photoanodes were carried out, and their Nyquist plots are shown in Figure 6. The semicircle sizes of Hier- and Mac-TiO_2 photoanodes are much smaller than that of Mes-TiO_2, indicating lower resistance of charge transfer between photoanode and electrolyte. Moreover, hierarchical sample presents higher photocurrent density in comparison to macroporous sample, which can be explained by the addition of mesopores provides more surface area for dye adsorption. Therefore, it is confirmed that hierarchical TiO_2 can improve photo to current conversion efficiency by combining the advantages of macropores and mesopores. Notably, Hier-TiO_2 shows much higher dye adsorption but only a few improvements in conversion efficiency. This conflict can be explained by the recombination of the photo-charges. Photoanode adsorbed more dyes generates more photoelectrons and photoholes under the solar light irradiation, but more photocharges have extra recombination opportunities, resulting in a drastic energy loss.

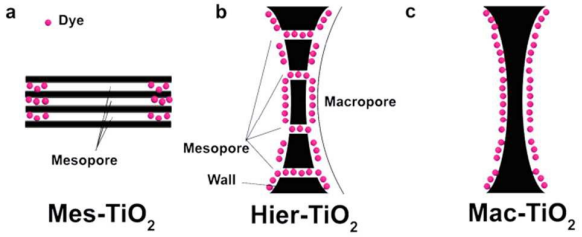

Figure 4. Models of dye adsorbed on different TiO_2 samples.

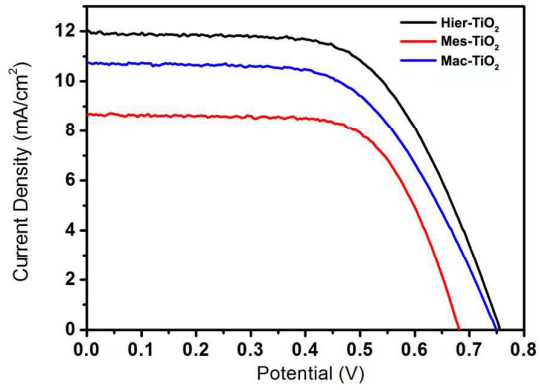

Figure 5. I-V curves of different DSSCs

Table 3. Parameters of different DSSCs

Sample	Mes-TiO_2	Mac-TiO_2	Hier-TiO_2
Voc (mV)	0.680	0.748	0.755
Jsc (mA/cm_2)	8.7	10.8	12.0
FF	0.67	0.58	0.60
η	4.0%	4.7%	5.4%

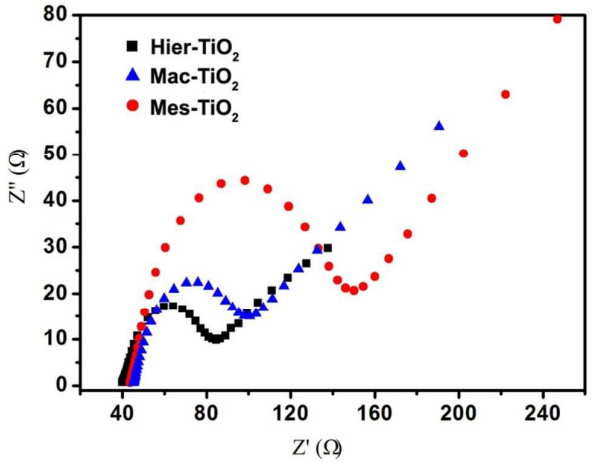

Figure 6. Electrochemical impedance spectroscopy (EIS) of the photoanodes.

Conclusions

We prepared a kind of hierarchical TiO_2 by using polystyrene spheres and F127 as template. Characterizations such as N_2 isotherms, XRD, and TEM proved macroporous and mesoporous structure both exsit in hierarchical TiO_2. What's

more, the charge collection effect of macroporous structure and large surface area of mesoporous morphology are combined to improve the photo to current conversion efficiency of DCCSs. Compared with mesoporous or macroporous TiO_2, the hierarchical sample shows superior DSSCs efficiency.

Corresponding Author

Jinlong Zhang* E-mail: jlzhang@ecust.edu.cn; Tel.:86-021-64252062
Lingzhi Wang* E-mail: wlz@ecust.edu.cn; Tel.:86-021-64252062

Acknowledgements

This work has been supported by the National Nature Science Foundation of China (21173077, 21377038 and 21237003, 21203062), the National Basic Research Program of China (973 Program, 2013CB632403), the Research Fund for the Doctoral Program of Higher Education (20120074130001) and the Fundamental Research Funds for the Central Universities.

Notes and references

The authors declare no competing financial interests.

1. M. GrÄtzel, *Accounts Chem Res*, 2009, **42**, 1788-1798.
2. B. O'Regan and M. Gratzel, *Nature*, 1991, **353**, 737-740.
3. S. Ito, T. N. Murakami, P. Comte, P. Liska, C. Grätzel, M. K. Nazeeruddin and M. Grätzel, *Thin Solid Films*, 2008, **516**, 4613-4619.
4. X. Chen, C. Li, M. Grätzel, R. Kostecki and S. S. Mao, *Chem Soc Rev*, 2012, **41**, 7909.
5. D. Cahen, G. Hodes, M. Grätzel, J. F. Guillemoles and I. Riess, *J Phys Chem B*, 2000, **104**, 2053-2059.
6. Q. Zhang and G. Cao, *J Mater Chem*, 2011, **21**, 6769-6774.
7. J.-Y. Liao, J.-W. He, H. Xu, D.-B. Kuang and C.-Y. Su, *J Mater Chem*, 2012, **22**, 7910.
8. U. Bach, D. Lupo, P. Comte, J. E. Moser, F. Weissortel, J. Salbeck, H. Spreitzer and M. Gratzel, *Nature*, 1998, **395**, 583-585.
9. Y. Zhang, Z. Xie and J. Wang, *Acs Appl Mater Interfaces*, 2009, **1**, 2789-2795.
10. J.-W. Shiu, C.-M. Lan, Y.-C. Chang, H.-P. Wu, W.-K. Huang and E. W.-G. Diau, *ACS Nano*, 2012, **6**, 10862-10873.
11. J. Y. Liao, B. X. Lei, Y. F. Wang, J. M. Liu, C. Y. Su and D. B. Kuang, *Chem-Eur J*, 2011, **17**, 1352-1357.
12. C. S. Rustomji, C. J. Frandsen, S. Jin and M. J. Tauber, *J Phys Chem B*, 2010, **114**, 14537-14543.
13. D. Kuang, J. Brillet, P. Chen, M. Takata, S. Uchida, H. Miura, K. Sumioka, S. M. Zakeeruddin and M. Grätzel, *ACS Nano*, 2008, **2**, 1113-1116.
14. W. Guo, C. Xu, X. Wang, S. Wang, C. Pan, C. Lin and Z. L. Wang, *J Am Chem Soc*, 2012, **134**, 4437-4441.
15. B. Liu and E. S. Aydil, *J Am Chem Soc*, 2009, **131**, 3985-3990.
16. J.-H. Shin and J. H. Moon, *Langmuir*, 2011, **27**, 6311-6315.
17. Z. Yang, S. Gao, W. Li, V. Vlasko-Vlasov, U. Welp, W.-K. Kwok and T. Xu, *Acs Appl Mater Interfaces*, 2011, **3**, 1101-1108.
18. N. Tétreault, É. Arsenault, L.-P. Heiniger, N. Soheilnia, J. Brillet, T. Moehl, S. Zakeeruddin, G. A. Ozin and M. Grätzel, *Nano Lett*, 2011, **11**, 4579-4584.
19. H.-Y. Chen, D.-B. Kuang and C.-Y. Su, *J Mater Chem*, 2012, **22**, 15475.
20. C.-Y. Cho and J. H. Moon, *Langmuir*, 2012, **28**, 9372-9377.
21. B. Mandlmeier, J. M. Szeifert, D. Fattakhova-Rohlfing, H. Amenitsch and T. Bein, *J Am Chem Soc*, 2011, **133**, 17274-17282.
22. E. J. W. Crossland, N. Noel, V. Sivaram, T. Leijtens, J. A. Alexander-Webber and H. J. Snaith, *Nature*, 2013, **495**, 215-219.
23. J.-Y. Liao, B.-X. Lei, D.-B. Kuang and C.-Y. Su, *Energ & Environ Sci*, 2011, **4**, 4079-4085.
24. Y. Zhang, A. H. Yuwono, J. Wang and J. Li, *J Phys Chem C*, 2009, **113**, 21406-21412.
25. D. Qi, L. Lu, Z. Xi, L. Wang and J. Zhang, *Appl Catal B: Environ*, 2014, **160**, 621-628.

TOC